

Adaptive ROI Generation for Video Object Segmentation Using Reinforcement Learning

Mingjie Sun^a, Jimin Xiao^{a,*}, Eng Gee Lim^a, Yanchu Xie^a and Jiashi Feng^b

^a*Xi'an Jiaotong-Liverpool University, Suzhou, China*

^b*National University of Singapore, Singapore*

ARTICLE INFO

Keywords:

model adaptation
video object segmentation
reinforcement learning
training accelerate

ABSTRACT

In this paper, we aim to tackle the task of semi-supervised video object segmentation across a sequence of frames where only the ground-truth segmentation of the first frame is provided. The challenges lie in how to online update the segmentation model initialized from the first frame adaptively and accurately, even in presence of multiple confusing instances or large object motion. The existing approaches rely on selecting the region of interest for model update, which however, is rough and inflexible, leading to performance degradation. To overcome this limitation, we propose a novel approach which utilizes reinforcement learning to select optimal adaptation areas for each frame, based on the historical segmentation information. The RL model learns to take optimal actions to adjust the region of interest inferred from the previous frame for online model updating. To speed up the model adaption, we further design a novel multi-branch tree based exploration method to fast select the best state action pairs. Our experiments show that our work improves the state-of-the-art of the mean region similarity on DAVIS 2016 dataset to 87.1%.

1. Introduction

Video object segmentation (VOS) [52, 28, 30, 31, 2, 7] is a fundamental problem in the computer vision field with many applications including video editing [1, 17], video surveillance [4, 51], and scene understanding [10, 26]. The objective of single target video object segmentation is to label each pixel as foreground or background in a given frame of a video sequence. Labeling these pixels, however, is difficult due to background clutter, illumination change, motion blur, deformation, and so on.

There are many kinds of segmentation methods including semi-supervised video object segmentation [35, 6, 55], unsupervised video object segmentation [22, 45, 20, 8, 27], interactive video segmentation [6, 48, 40, 49, 19, 41, 37] and so on. For semi-supervised segmentation, the ground-truth annotation for each pixel of the first frame is provided. The segmentation model identifies pixels of foreground and background for the following frames.

Most recent approaches addressing semi-supervised video object segmentation are based on convolutional neural networks. In particular, the one-shot video object segmentation (OSVOS), introduced by Cacells et al. [5] has achieved great success. The core idea is to fine-tune an ImageNet [12] pre-trained ConvNet on the video object segmentation dataset, such as DAVIS [36, 38], to allow the segmentation model to find general objects in a frame at first. Then, the first frame of the inference video sequence will be used to fine-tune the segmentation model such that it can rapidly focus on the specified target object instance in the first frame. Despite the promising result obtained using OSVOS, such a method is challenged by the cases where the appearance of the tar-

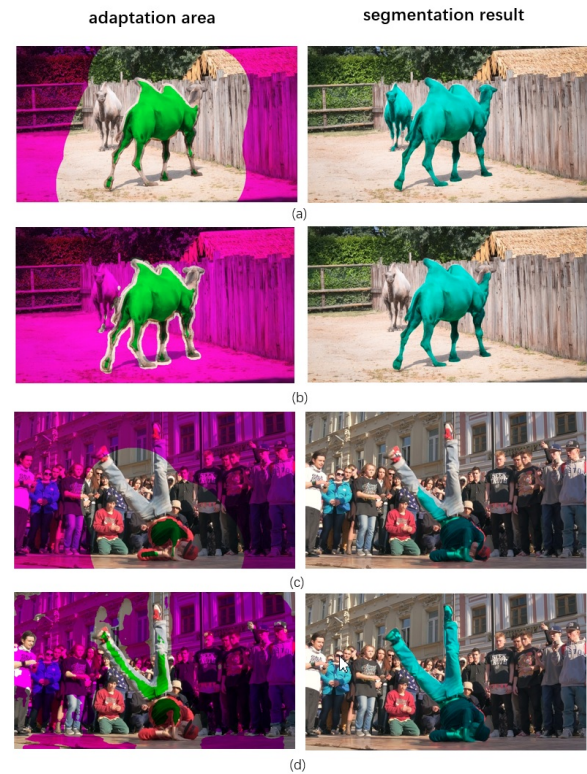


Figure 1: Different adaptation areas lead to different frame segmentation results. The segmentation models are the same before online adaptation. In the left column, the area in green is the adaptation area for foreground and the area in purple is the adaptation area for background.

get object changes dramatically in the video sequence and there may exist multiple confusing instances of similar appearance. OSVOS only learns the target object appearance

*Corresponding author

✉ mingjie.sun18@xjtlu.edu.com (M. Sun); jimin.xiao@xjtlu.edu.com (J. Xiao)

ORCID(s): 0000-0002-3697-7927 (M. Sun)

from the first frame of a video sequence. It cannot adapt to the target object appearance variation when deformation occurs or the camera rotates.

Inspired by the fact that the online adaption has achieved great progress on video object tracking at bounding box level [53, 29, 16, 9, 3, 11, 57], some works start to deploy the online adaption to video object segmentation. For instance, online adaptation video object segmentation (OnAVOS) [47] proposes an online adaptive video object segmentation meth-

od which enables to update the segmentation model during inference time. However, model drift may interrupt the model online adaptation and lead to performance drop.

We observe that, for online VOS model update, how to identify to the region of interest (ROI) for model adaptation is critical. In particular, as can be observed in Figure 1, if we select the adaptation area in a rough way, the segmentation model after adaptation performs very poor when there are multiple similar objects in the frame, especially, the distraction object is very close to the target. As such selecting the optimal adaptation area in a more sophisticated and flexible way is very significant for video object segmentation.

To tackle this problem, we formalize VOS as a conditional decision-making process where two reinforcement lea-

arning (RL) agents are employed to infer and adjust the ROI for adaption for both foreground and background in a flexible way. At each frame, the RL agent outputs actions to tune the ROI. Provided with such regions, the VOS model can be updated to be more specific and discriminating for the instance in the current frame.

To select the optimal adaptation area for video object segmentation, a set of features of different adaptation areas of the current frames will be fed into the RL model. Then, the RL model will select the best action, and to choose the most suitable adaptation area for the current frame. As a result, the segmentation model can obtain an accurate segmentation result. Though RL method is promising for region identification, it is notoriously slow to optimize the agent. In this work, to speed up the RL agent training, we propose a multi-branch tree based policy search method where possible action state pairs are organized in a tree structure.

To sum up, this paper has three main contributions:

- We observe the importance of identifying the ROI for VOS model adaptation and make the attempt to mine optimal adaptation areas for online adaptation in video object segmentation. Specifically, we deploy the “actor-critic” RL framework to train the agent for generating the adaptation areas.
- Both VOS with online adaptation and the RL model training are computational demanding processes. To speed up the RL training, we further design a novel multi-branch tree based exploration method to fast select the best state action pairs.
- The proposed approach has been validated on DAVIS 2016, SegTrack V2 and Youtube-Object dataset. New

state-of-the-art result of mean region similarity is obtained for the DAVIS 2016 dataset, which is 87.1%.

2. Related Work

2.1. Video Object Segmentation

Recently, with the popularity of deep neural network, various deep learning based video object segmentation models have been proposed. These existing approaches can be classified into three different categories, including unsupervised methods, weakly supervised methods and semi-supervised methods. Unsupervised methods and weakly supervised methods are more difficult than semi-supervised methods because no pixel-level annotations are available. Utilizing motion information and detecting the primary object in a frame are two common ways to address this problem. In [45], Pavel et al. combine the object appearance information and the motion information together successfully and achieve a good performance. In [43], Song et al. propose to use concatenated pyramid dilated convolution features and dramatically improve the final accuracy.

Semi-supervised video object segmentation task, where the pixel-level annotation of the first video frame is available, is also an extensively studied task. The most common approach for this task is to pre-train a general segmentation network. Then, the network is fine-tuned using the first frame annotation to enable the network focusing on the particular object in the frame [5]. In order to adapt to object appearance variation, a novel approach to update the segmentation network during test time is proposed in [47]. In [30], another method is proposed where proposals will be generated first, and then they will be merged into accurate and temporally consistent pixel-wise object tracks. In [2], this task is viewed as a spatio-temporal Markov random field problem, and ConvNet is utilized to encode the dependencies among pixels. To overcome the shortage of training data, it is proposed to use static images to generate additional training samples in [54]. In [34], Everingham et al. attempt to utilize the part-based tracking method to generate bounding box and segmentation for each part. In [56], Xiao et al. apply meta learning to video segmentation and dramatically speeds up the segmentation process.

Different from the existing works, we formulate the selection of ROI for online segmentation adaptation as a Markov decision process and utilize the RL to address this problem.

2.2. Deep Reinforcement Learning

RL algorithm learns to achieve a complex objective from past experience. “actor-critic” [23] is a popular RL framework that inherits several previous RL frameworks including deep Q-learning [33] and policy gradient [44] which are valued-based and policy-based strategies, respectively.

RL has been applied to many areas of computer vision, in particular for visual object tracking at bounding box level. In [58], Yun et al. use RL to choose sequential actions to move the bounding box step by step from the original object location in the previous frame to correct location. In [18],

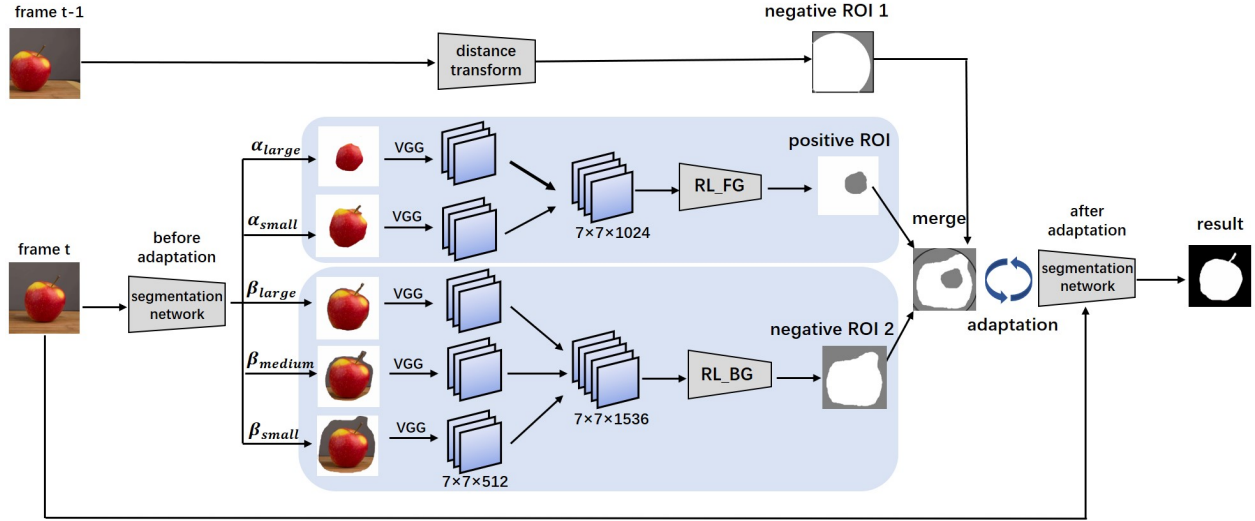


Figure 2: The network architecture of our work consists of two RL models. One is to choose the adaptation area for foreground, and another is to choose the adaptation area for background. We use pre-trained VGG19 model to extract the feature of each ROI area of the current frame, and then feed the combined feature into the RL model as the state. Finally, the RL model will choose the best adaptation area and update the segmentation model using the chosen adaptation area.

Huang et al. propose a novel RL based model which can choose the most suitable number of deep convolutional layers according to the current frame complexity, which dramatically reduces the running time. In [13], Dong et al. propose to deploy the RL to choose the optimal hyper-parameter for correlation filter.

In pixel-level video object segmentation, to the best of our knowledge, however, there is only one attempt to apply RL to this task. Han et al. establish a novel RL framework which can choose the optimal object box and the context box [15]. This work is motivated by the observation that, for an identical segmentation model, different object boxes and context boxes generate different segmentation masks. Thus, it is natural to utilize RL to choose an optimal object-context box pair to achieve the best segmentation result.

Different from the existing work [15], our work aims to utilize the RL to choose the optimal ROI to update the segmentation network during test time.

3. Our Approach

3.1. Overview

In general, the main objective of our work is to utilize RL to improve the performance of video object segmentation with online adaptation. Different from the existing approaches to select the adaptation ROI in a rough way, our work utilizes RL to choose the optimal adaptation ROI for each individual frame to avoid model drift. In other words, different frames will own its particular standard to choose adaptation ROI. The overview diagram of our proposed method is described in Figure 2.

3.1.1. VOS with Online Adaptation

Our work is built on the top of VOS model with online adaptation. Before finally segmenting the current frame F_t

of a video sequence, a part of pixels in F_t will be used to update the current segmentation model to adapt to the change of the foreground and background. These pixels consist of positive ROI regarded as foreground, denoted as S_p , and the negative ROI regarded as background, denoted as S_n . In On-AVOS [47], S_p and S_n are chosen according to two fixed thresholds including T_p and T_n . In order to determine S_p , F_t will be fed into the segmentation model and a temporary (before online adaptation) probability map M_f , whose size is the same as the F_t , will be generated. In M_f , for a pixel i , $M_f(i)$ refers to the probability that pixel i belongs to the foreground of F_t . Then, S_p will be chosen according to T_p , as follows:

$$S_p = \{i | i \in F_t, M_f(i) > T_p\}. \quad (1)$$

Negative ROI S_n is decided by the distance to the positive ROI S_p . S_n are the pixels far away from S_p , as follows:

$$S_n = \{i | i \in F_t, distance(i) > T_n\}, \quad (2)$$

where $distance(i)$ refers to the distance of pixel i to S_p .

3.1.2. RL Based Online Adaptation

Existing VOS methods with online adaptation, i.e., On-AVOS [47], adopt a fixed standard to select the adaptation area, including T_p and T_n , where different characteristics of each frame are not considered. To address this problem, we use flexible thresholds, t_p and t_n , to choose the adaptation ROI. We build two RL models to choose the most suitable t_p and t_n for each frame.

Our RL framework includes state $s \in S$, threshold selection action $a^p \in A^p$ to determine the value of t_p and threshold selection action $a^n \in A^n$ to determine the value of t_n , state transition function $s' = T(s, a^p, a^n)$ and the reward function $g(s, a^p, a^n)$. Given a frame F_t of one sequence, first

of all, F_t will be fed into the segmentation network to obtain a temporary probability map M_f . A set of ROIs can be obtained according to the candidate thresholds. In our work, we need 5 ROIs where the probability value is greater than α_{large} , α_{small} , β_{large} , β_{medium} and β_{small} , respectively. Note that β_{micro} is ignored to diminish the complexity of the state. The first two ROIs are used for the RL model to choose t_p while the last three ROIs are used for RL model to choose t_n . In other words, the possible values of t_p can be α_{large} or α_{small} , and the possible values of t_n can be β_{large} , β_{medium} , β_{small} or β_{micro} . After t_p and t_n are determined, pixels with probability values greater than t_p will be viewed as the adaptation ROI for foreground, as follows:

$$S_p = \{i | i \in F_t, M_f(i) > t_p\}, \quad (3)$$

while these pixels with probability value less than t_n , combined with the negative pixels chosen by distance using (2), will be regarded as the adaptation ROI for background, as follows:

$$S_n = \{i | i \in F_t, distance(i) > T_n\} \cup \{i | i \in F_t, M_f(i) < t_n\}. \quad (4)$$

S_p and S_n are used to update the current segmentation model while other pixels are ignored. After the segmentation model has been updated, F_t will be fed into the new segmentation network and the final segmentation result is obtained.

The pseudo-code of our algorithm is described in Algorithm 1.

Algorithm 1: RL Based Video Object Segmentation

Input:

Ground-truth of the first frame $gt(1)$
Sequence length L
Distance threshold T_n
Segmentation network Seg_Net
Pretrained VGG network VGG
RL model to choose positive threshold RL_p
RL model to choose negative threshold RL_n

Output: Segmentation result of Frame t O_t

Fine-tune Seg_Net on F_1
 $last_mask \leftarrow gt(1)$
for $t = 2$ to L **do**
 Obtain 2 RL states using (5) and (6), respectively.
 Feed the states into the RL models and achieve the optimal threshold t_p and t_n .
 Obtain positive ROI and negative ROI using (3)(4), respectively.
 Update Seg_Net on F_t using S_p and S_n .
 $O_t \leftarrow forward(Seg_Net, F_t) > 0.5$
 $last_mask \leftarrow O_t$
end

3.2. Agent Action

The framework of our work consists of two RL models, including one to choose t_p and another to choose t_n , as shown

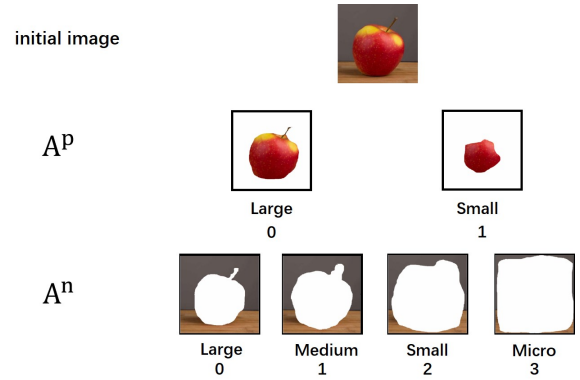


Figure 3: Foreground adaptation ROI selecting action set A^p and background adaptation ROI selecting action set A^n .

in Figure 3. The action set A^p used for the first RL model to choose S_p contains 2 candidate thresholds: α_{large} and α_{small} . As the difference of the ROI areas with different t_p is not very big, we only set two candidate thresholds for the action set A^p . The action set A^n used for the second RL model to choose S_n contains 4 candidate thresholds: β_{large} , β_{medium} , β_{small} and β_{micro} . As the size of S_n is much larger than that of S_p , we set more candidate thresholds for t_n .

In terms of the design of the candidate values of t_p , in OnAVOS [47], T_p is 0.97 and it is fixed for all frames. This threshold is very safe and conservative because it should work in any situation, especially for some frames with very bad segmentation result. In fact, for some frames with good segmentation result, the value of t_p ought to be much lower, so more correct pixels of the object can be used to update the model and improve the final segmentation result. As the difference of the size of the adaptation ROIs with different t_p is not very huge, we only set two candidate thresholds for the action set A^p , which can lower the difficulty of training the RL model.

In terms of the design of the candidate values of t_n , in OnAVOS [47], S_n are chosen according to the distance to the target object rather than the value of the M_f . If a pixel is far away from the target, it will be viewed as S_n . Similarly, the selection of S_n in OnAVOS [47] is very conservative as it works for almost all frames. In our work, we still keep the adaptation ROI which are chosen by the distance, and then try to add more areas to include more correct adaptation ROI for background. The additional area is chosen by the value of M_f . Finally, we combine these two parts of areas together as the final area of S_n using (4). As the size of the area for S_n is much larger than the area of S_p , we set more candidate thresholds for t_n .

In this way, after training, these two RL models can choose the best action and achieve the optimal thresholds t_p and t_n .

3.3. State and Reward

The state s is the input of the RL model. As we have two RL models, we need two sets of states for two models. In

general, the state s is a feature map combined by the feature maps of different candidate adaptation ROIs where the probability value of all pixels in a certain adaptation ROI is less than a certain threshold.

First, given a certain frame F_t , we feed F_t into the segmentation model before test time adaptation and generate the temporary probability map M_f . Then, we generate 5 ROIs with 5 different candidate thresholds according to the value of M_f . The ROIs where the probability values of all pixels in this area are greater than α_{large} and α_{small} , receptively, are combined as the state of the RL model to choose t_p , as follows,

$$state_p = feature(\{i|i \in F_t, M_f(i) > \alpha_{large}\}) + feature(\{i|i \in F_t, M_f(i) > \alpha_{small}\}). \quad (5)$$

The ROIs where the probability values of all pixels in this area are greater than β_{large} , β_{medium} and β_{small} , receptively, are combined as the state of the RL model to choose t_n , as follows,

$$state_n = feature(\{i|i \in F_t, M_f(i) > \beta_{large}\}) + feature(\{i|i \in F_t, M_f(i) > \beta_{medium}\}) + feature(\{i|i \in F_t, M_f(i) > \beta_{small}\}). \quad (6)$$

Note that β_{micro} is ignored in (6) to diminish the complexity of $state_n$, as $feature(\{i|i \in F_t, M_f(i) > \beta_{small}\})$ already provides sufficient information to help the RL model make the decision. We use the VGG model [42], pre-trained on the ImageNet classification dataset [12], to extract the features of these ROIs first. Then, we concatenate these features together as the state of the RL model. We use the first 5 convolutional blocks of the VGG19 model which results in a feature size of $\mathbb{R}^{7 \times 7 \times 512}$ for one ROI. For the RL model to choose t_p , the features of two ROIs will be concatenated to generate the final state $s_{t_p} \in \mathbb{R}^{7 \times 7 \times 1024}$. For the RL model to choose t_n , the features of three ROIs will be concatenated to generate the final state $s_{t_n} \in \mathbb{R}^{7 \times 7 \times 1536}$. Finally, states s_{t_p} and s_{t_n} will be fed into the corresponding RL model and result in the actions to choose the optimal thresholds t_p and t_n .

The reward function is defined as $r_t = g(s_t, a_p, a_n)$ which reflects the performance of the final segmentation result of each frame in the video sequence:

$$g(s_t, a_t, a_n) = \begin{cases} IOU + 1 & IOU > 0.1 \\ -1 & IOU \leq 0.1 \end{cases}, \quad (7)$$

where IOU indicates the intersection-over-union (IOU) between the prediction and the ground-truth, which reflect the quality of the predicted segmentation.

3.4. Training in Actor-Critic Framework

In our work, we adopt the ‘‘actor-critic’’ framework [23] for RL training. In general, one ‘‘actor-critic’’ framework consists of two roles including an ‘‘actor’’ role to generate an action and a ‘‘critic’’ role to measure how good this action is.

In this work, we need to select the optimal adaptation ROIs for both foreground and background separately. Therefore, we need two ‘‘actor-critic’’ model pairs, including one ‘‘actor-critic’’ pair for foreground, and another pair for background. Four individual RL models are deployed in total.

In our ‘‘actor-critic’’ framework, given a current frame F_t , the first step is to feed the state into the ‘‘actor’’ network and generate an action a , which is to choose the optimal adaptation ROIs. The corresponding reward r_t will also be obtained after conducting this action. r_t is decided by the IOU of the segmentation result according to (7).

In the training process, after the forward process, the ‘‘critic’’ network will be updated first in the valued-based way, as follows:

$$w = w' + \alpha * \delta_t \nabla_{w'} V_{w'}(s_t), \quad (8)$$

where

$$\delta_t = r_t + \gamma * V_{w'}(s_{t+1}) - V_{w'}(s_t). \quad (9)$$

In (8) and (9), w and w' indicate the weight of the ‘‘critic’’ model after and before update. α is the learning rate of the ‘‘critic’’ model. δ_t is the TD error which indicates the difference of the actual score and the predicted score. $V_{w'}(s_t)$ refers to the accumulated reward of state s_t which is predicted by the ‘‘critic’’ model before update. γ refers to the discount factor.

After the ‘‘critic’’ model has been updated, the ‘‘actor’’ model will be updated in a policy-based way, as follows:

$$\theta = \theta' + \beta * \nabla(\log \pi_{\theta'}(s_t, a_t)) * A(s_t, a_t), \quad (10)$$

where $A(s, a)$ refers to the advantage function, and $A(s_t, a_t) = \delta_t$ according to (9), θ and θ' indicate the weight of the ‘‘actor’’ model after and before update. β is the learning rate of the ‘‘actor’’ model. Policy function $\pi(s, a)$ is a network whose input is the state s and a certain action a , and output is the probability of selection action a in state s .

In this way, when training the RL models, our ‘‘actor-critic’’ framework can avoid the shortage of value-based and policy-based methods. Instead of waiting until the end of the episode, our RL models can be updated at each step, which dramatically reduces the training time but maintains the RL training stability.

4. Implementation Details

4.1. Train the Segmentation Network

The proposed method trains the segmentation network follows the strategy of [5] and [47]. The first step is to train a ImageNet pre-trained network on a pixel-level annotated dataset such as PASCAL VOC [14]. In the second step, we use the DAVIS video dataset [36] to train the network so that the network is able to adapt to this dataset. We also fine-tune the network on the first frame of DAVIS test videos whose ground-truth annotation is provided. In this way, the segmentation network is well trained and can achieve a good result before test time adaptation.

4.2. Train the RL Model

Before training the RL model, the related data need to be stored in advance to accelerate the training process, which will be described in section 4.3. In terms of the training of the RL models, specifically, we divide all video sequences in DAVIS 2016 training set into video clips with the fixed number of frames. A video clip includes 10/5 consecutive frames is used as a sample for the RL model to select foreground/background ROI. Using stored clips for training dramatically reduces the training time of the RL model.

We randomly select 20 clips as a batch for training the RL models. At the beginning of the training, the learning rate α for “actor” model is $1e-5$, and the learning rate β for “critic” model is $5e-5$. The learning rate decreases gradually during the training, and it decreases by 1% for each 200 iterations. The discount rate γ for the reward is 0.9. In terms of values for candidate threshold t_p and t_n , we found $\alpha_{large}=0.97$, $\alpha_{small}=0.7$, $\beta_{large}=0.4$, $\beta_{medium}=0.2$, $\beta_{small}=0.1$ and $\beta_{micro}=0.01$ works well through cross validation. The training of our RL models takes about 3 days on a NVIDIA GTX 1080 Ti GPU and a 12 Core Intel i7-8700K CPU@3.7GHz.

4.3. Accelerating RL Training

Segmentation with online adaptation is slow because the segmentation model should be updated for each frame. Meanwhile, RL training itself is also slow. Training the RL model heavily relies on a large number of attempts for different actions. Normally, to generate a well trained RL model, the model should be trained with more than one million iterations. If the running time for each training process is too long, the total time is unbearable. Thus, it is impossible to train the RL model in a regular way.

To address this issue, inspired by the idea of sacrificing space to improve efficiency, we propose a novel multi-branch tree structure, as shown in Figure 4, to store all possible segmentation results using different adaptation ROIs into a repository in advance. Training an “actor-critic” framework needs 4 types of information including the action, the reward, the states before and after the action. For each node in the multi-branch tree, a corresponding directory is generated. The image of the frame, the temporary probability map and the IOU of the segmentation result after executing a certain action are stored as files. All possible actions are stored as a links to next layer of nodes. In this way, the image and the probability map are used to generate the state. The IOU value is used to generate the reward. Finally, this repository will be organized in a multi-branch tree structure, whose stored data will be used to update the RL model during the process of training using the method described in section 3.4.

5. Experiments

5.1. Experiment Setup

Our method is evaluated on three widely-used datasets including the DAVIS 2016 dataset [36], Youtube-Object dataset [39] and Segtrack V2 dataset [25]. DAVIS 2016 dataset consists of 50 high quality video sequences and 3,455 frames,

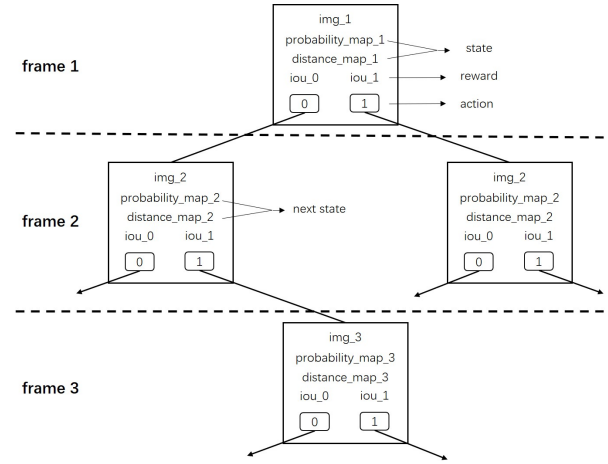


Figure 4: The data structure used to restore the related data to accelerate the RL model training. For RL model to select the t_n , distance map is required for the training, while the training for the RL mode to selected t_p does not need it.

spanning multiple occurrences of common video object segmentation challenges such as occlusions, motion-blur and appearance changes. 30 video sequences of DAVIS 2016 are used for training, and 20 video sequences are used for testing. In DAVIS 2016, in each video sequence, only a single object instance is annotated. DAVIS 2017 dataset [38] extends the DAVIS 2016 dataset where multiple objects, rather than only one object, are annotated in each frame. As our method targets for single instance segmentation, we only do the experiment on DAVIS 2016. In Youtube-Object, there are 155 video sequences and a total of 570,000 frames. These video sequences are divided into 10 classes. Training set and testing set are not separated in Youtube-Object dataset so it is only used for testing. In SegTrack V2 dataset, there are 14 video sequences with more occlusion than appearance changes compared with Youtube-Object dataset.

We evaluate our method following the approach proposed in [36]. The adopted evaluation metrics include region similarity J and contour accuracy F . The region similarity is calculated as $J = \left| \frac{m \cap gt}{m \cup gt} \right|$ by the intersection-over-union between the predicted segmentation m and the ground-truth gt . The contour accuracy is defined as $F = \frac{2P_c R_c}{P_c + R_c}$, which indicates the trade-off between counter-based precision P_c and recall R_c .

5.2. Comparison with State-of-the-arts

In this section, we will compare our proposed work with other state-of-the-art semi-supervised video object segmentation methods, including PReMVOS [30], OnAVOS [47], CINM [2], LucidTracker [21], MSK [35], OSVOS [5], STV [50], ObjectFlow [46]. Note that OSVOS-S [31] is not included in the comparison list as it utilizes additional dataset for training.

Table 1 summarizes the quantitative results of recent methods on the DAVIS 2016 validation set consisting of 20 videos.

Method	DAVIS-16 J_m	DAVIS-16 F_m	SegTrack V2 J_m	Youtube Objs J_m	t(s)
PRemVOS [30]	84.9	88.6	-	-	30
OnAVOS [47]	<u>85.7</u>	84.8	66.7	77.4	13
CINM [2]	83.4	85.0	77.1	<u>78.4</u>	120
Lucid [21]	83.7	-	76.8	76.2	40
MSK [35]	79.7	75.4	72.1	75.6	12
OSVOS [5]	79.8	80.6	65.4	78.3	10
STV [50]	73.6	-	78.1	-	-
ObjFlow [46]	68.0	-	74.1	77.6	-
OURS	87.1	<u>86.1</u>	<u>77.5</u>	79.5	14

Table 1

Quantitative comparison with other methods on the DAVIS 2016, SegTrack V2 and Youtube-Object dataset. For J_m and F_m , the method with the best performance is bold, and the method with the second best performance is marked with underline.

Method	DAVIS 2016
WO adaptation	80.3 \pm 0.4
foreground adaptation	82.1 \pm 0.5
background adaptation	85.3 \pm 0.5
full adaptation	86.5 \pm 0.4
full adaptation + CRF	87.1 \pm 0.4
OnAVOS [47] WO CRF	84.6 \pm 0.6
OnAVOS [47]	85.7 \pm 0.6
CINM [2]	84.2

Table 2

Ablation study on the contribution of individual RL model for the DAVIS 2016 dataset, measured by the mean region similarity J_m . WO indicates without.

Method	SegTrackV2
WO adaptation	61.4 \pm 0.6
foreground adaptation	66.2 \pm 0.5
background adaptation	73.2 \pm 0.5
full adaptation	76.6 \pm 0.5
full adaptation + CRF	77.5 \pm 0.5
OnAVOS [47] WO CRF	64.9 \pm 0.6
OnAVOS [47]	66.7 \pm 0.6
CINM [2]	77.1

Table 3

Ablation study on the contribution of individual RL model for the SegTrack V2 dataset, measured by the mean region similarity J_m . WO indicates without.

The top 3 performing methods have been highlighted with different colors. It can be observed that our work has achieved outstanding result under both mean region similarity J_m and the mean contour accuracy F_m . Especially on mean region similarity J_m , our method achieves the best result which outperforms any existing state-of-the-art methods. Compared with the most competitive and related method OnAVOS [47], our method improves the mean region similarity J_m to 87.1%. It should be noted that the gain over [47] is solely due to the fact that better ROIs are obtained for online adaptation using RL. Note that, same to [32], according to the randomness of the segmentation network, the final accuracy may fluctuate around 0.4%. The proposed mean region similarity J_m is the average value from experiments of 10 times.

Figure 5 shows the qualitative segmentation masks for different methods. As can be observed, our method performs better on videos with significant appearance change for the target object, for instance, the camel and breakdance video sequences. Especially when multiple similar objects are close to each other, e.g., the camel sequence, our method has the ability to distinguish the target object from other similar objects successfully.

On SegTrack V2 and Youtube-Object datasets, as training set and evaluation set are not split, all video sequences are used for evaluation. From Table 1, we can observe that

our method also performs well on both datasets. Compared with OnAVOS [47], our method improve the mean region similarity J_m by 10.8% on SegTrack V2 dataset, which demonstrates the effectiveness of our RL models to choose the online adaptation ROIs. In addition, our approach also improves the mean region similarity J_m by 2.1% on Youtube-Object dataset. This result can show the robustness of our method on different evaluation datasets.

In addition, we compare our run time with other state-of-the-art methods, and the result is also reported in Table 1. Despite the fact that we improve the mean region similarity J_m of our baseline method with online adaptation [47] by 10.8% on SegTrack V2 dataset and 1.4% on Davis 2016 dataset, the run time of our method is only about 1 second longer than [47], which demonstrates the efficiency of our method.

5.3. Ablation studies

In this section, we conduct four ablation studies on our method using the testing video sequences of DAVIS 2016 dataset and SegTrack V2 dataset.

We conduct the first ablation studies on the DAVIS 2016 and SegTrack V2 datasets, where parts of our method are disabled to investigate the impact of each component. In this study, we also explore the contribution of each individual RL

model in our method, one of these two RL models is disabled during this ablation study respectively, and the results will be compared with the result generated by the method with full RL models. Table 2 shows the result of this ablation study on the DAVIS 2016 dataset. On the DAVIS 2016 dataset, when using both foreground and background adaptation, we obtain the mean region similarity J_m of 86.5% without CRF [24]. J_m of our method with full adaptation is greater than the method without any adaptation by 6.2%, which demonstrates the effectiveness of our online adaptation approach. In addition, compared with the rough approach to choose the adaptation ROI adopted by OnAVOS [47], before CRF, our method is also 1.9% greater than it. After executing CRF, the gain degrades a little to 1.4%, which demonstrates that our flexible way to choose the optimal adaptation ROI for each frame is significant for the final segmentation result. To study the individual influence of each RL model, we remove the RL model to choose the optimal adaptation ROI for background, obtaining the method **foreground adaptation**, and remove the model to choose the adaptation ROI for foreground, obtaining the method **background adaptation**. As can be observed from the Table 2, using **foreground adaptation** method and **background adaptation** method obtains J_m of 82.1% and 85.3% on DAVIS 2016 dataset, respectively, which indicates that both RL models improve the segmentation result while the RL to choose the optimal adaptation ROI for background makes larger contribution to the final segmentation result. This observation also explains the reason why we have more threshold candidates for background than foreground. We also conduct the same ablation studies on the Segtrack V2 dataset and obtain the similar results as can be observed from the Table 3. When using both foreground and background adaptation, we obtain J_m of 61.4% without CRF. J_m of our method with full adaptation is greater than the method without any adaptation by 15.2%. The comparison between the rough approach to choose the adaptation ROI adopted by OnAVOS [47] and the proposed method is conducted on Segtrack V2 dataset as well, before CRF. The result is that J_m of the proposed method is 11.7% greater than the baseline method, which is a dramatic improvement of the mean region similarity. After the process of CRF, the gain degrades a little to 10.8%, which is still a huge improvement. To study the individual influence of each RL model on Segtrack V2 dataset, we also adopt the method **foreground adaptation** and the method **background adaptation**, as on the DAVIS 2016 dataset. As can be observed from the Table 3, using **foreground adaptation** method and **background adaptation** method obtains 66.2% and 73.2% J_m on Segtrack V2 dataset, respectively, which also indicates that both of the two RL models contribute to the improvement of segmentation result. This experiment also demonstrates the importance of the optimal adaptation ROI mining.

The purpose of the second ablation experiment is to demonstrate that it is important to select different t_n and t_p for each specific frame, rather than adopting a particular fixed set of thresholds. In other words, no matter which set of t_n

t_n	t_p	J_m
0.4	0.97	61.9 \pm 0.6
0.4	0.7	61.2 \pm 0.6
0.2	0.97	64.2 \pm 0.6
0.2	0.7	62.5 \pm 0.6
0.1	0.97	73.7 \pm 0.6
0.1	0.7	69.6 \pm 0.6
0.01	0.97	83.6 \pm 0.6
0.01	0.7	80.1 \pm 0.6
OURS		87.1 \pm 0.4

Table 4

Performance comparison between heuristic adaptation ROIs selection and RL-based adaptation ROIs selection, conducted on the DAVIS 2016 dataset, measured by the mean region similarity J_m . t_n indicates the threshold to choose the adaptation ROI for background. t_p indicates the threshold to choose the adaptation ROI for foreground.

and t_p are chosen, as long as these thresholds are fixed for all frames, the final segmentation result will be worse than the result generated by adopting the optimal thresholds selected by the RL models for each specific frame. More specifically, the RL model to select the adaptation ROI for background has 4 candidate thresholds including {0.4, 0.2, 0.1, 0.01}. The RL model to select the adaptation ROI for foreground has 2 candidate thresholds including {0.97, 0.7}. In this way, there are totally 8 possible combinations of t_p and t_n , which are listed in Table 4. In this experiment, each combination of t_n and t_p is adopted as the fixed thresholds for the segmentation model adaptation and its corresponding result is evaluated and compared with the result generated by the proposed method. As can be observed from Table 4, among these combinations, the most "conservative" one, i.e. $t_p=0.97$ and $t_n=0.01$ performs best. Note that these values are different from the final result of OnAVOS[47] because OnAVOS selects the background adaptation ROI according to the distance, rather than the value of the probability map. The performance decreases dramatically when the value of the fixed threshold gets close to 0.5 because the error of segmentation will propagate quickly when adopting these "greedy" thresholds for all frames. The highest obtained J_m (83.6 %) of the method adopting fixed thresholds, however, is still much lower than the result generated the proposed method (87.1 %). According to the observation of this experiment, it is obvious that the improvement does result from the RL models that choose the optimal t_n and t_p for each individual frame, rather than the contribution of a certain fixed combination of t_n and t_p .

The purpose of the third ablation experiment is to demonstrate that the proposed method is able to find a better adaptation ROI, compared with the baseline method. The metric to evaluate the selected adaptation ROI is the IOU between the adaptation ROI and the ground-truth. In this way, we firstly calculate the IOU between the adaptation ROI selected by the RL model and ground-truth. Then, we calculate the IOU between the adaptation ROI selected by the baseline method

Video	IOU-B-RL	IOU-B-Base	IOU-F-RL	IOU-F-Base	J_m -RL	J_m -Base	Δ IOU-B	Δ IOU-F	ΔJ_m
blackswan	99.4	44.6	91.0	74.6	95.4	95.4	54.8	16.4	0
bmx-trees	98.9	75.1	39.9	15.6	55.5	52.5	23.8	24.3	3.0
breakdance	97.4	55.9	74.9	55.0	80.2	68.4	41.5	19.9	11.8
camel	98.8	45.0	89.9	70.8	93.8	84.0	53.8	19.1	9.8
car-roundabout	99.4	41.8	95.2	85.4	97.1	97.1	57.6	9.8	0
car-shadow	99.7	60.1	92.7	79.2	96.1	96.0	39.6	13.5	0
cows	99.1	43.1	91.6	76.9	94.6	94.6	56.0	14.7	0
dance-twirl	98.1	59.3	83.3	63.2	87.3	84.6	38.8	20.1	2.7
dog	99.3	52.6	92.6	78.9	95.1	95.1	46.7	13.7	0
drift-chicane	99.6	72.1	83.0	55.6	89.1	87.2	27.5	27.4	1.8
drift-straight	99.1	64.4	90.1	75.8	92.7	91.3	34.7	14.3	1.3
goat	99.0	58.4	88.8	73.7	91.2	91.1	40.6	15.1	0
horsejump-high	98.9	61.8	80.0	52.4	87.3	86.8	37.1	27.6	0.5
kite-surf	98.3	72.4	57.2	28.0	66.7	66.7	25.9	29.2	0
libby	99.3	66.3	74.9	45.1	86.1	86.1	33.0	29.8	0
motocross-jump	93.9	41.2	87.5	70.7	90.4	86.4	52.7	16.8	4.0
paragliding-launch	97.1	69.1	58.7	44.9	62.5	62.5	28.0	13.8	0
parkour	99.4	67.3	85.1	61.7	91.8	91.4	32.1	23.4	0.4
scooter-black	98.6	58.2	86.1	68.1	89.8	89.0	40.4	18.0	0.8
soapbox	98.3	46.1	86.0	65.4	90.1	86.2	52.2	20.6	3.8
mean	98.6	57.7	81.4	62.0	86.5	84.6	40.9	19.4	1.9

Table 5

Quality comparison between the selected ROIs of the proposed method and the baseline method, as well as their influences on the final segmentation results, conducted on the DAVIS 2016 dataset, measured by the mean region similarity J_m . In this table, IOU indicates the IOU between the adaptation ROI selected and the ground-truth. J_m indicates the mean region similarity. B refers the background and F refers to the foreground. RL refers to the RL model and Base refers to the baseline method. Δ refers the difference value between the RL model and the baseline method. All values in this table are calculated before CRF.

and the ground-truth. Finally, we compare these two IOUs and their contributions to the final final segmentation result. As can be observed from Table 5, on average, the IOU of the proposed method is 40.9 % and 19.4 % higher than the baseline method, for background and foreground respectively. This result also coincides with the facts reported in Table 2 and Table 3 that background ROI adaptation using RL brings more performance gain than foreground ROI adaptation. Finally, as more correct pixels are adopted to update the segmentation model in the proposed method, the segmentation model is able to properly adjust itself to the change of the target in the video. It is also the reason why the proposed method can achieve improvement on the final segmentation result.

The fourth ablation experiment is to study the influence of different states for the RL model. The adopted state for the RL model also greatly affects the convergence difficulty of the training process as well as the final segmentation performance. We design three different states to study this factor. The first state is to feed the initial image (3 channels) and the temporary probability map (1 channel) into a train-from-scratch ConvNet without using pre-trained VGG model. This is because the input of the VGG model should be a 3-channel image. The second one is to feed the initial image (3 chan-

nels) concatenated with several mask channels to indicate different adaptation area, similarly, without the feature extracting of VGG model. The third one is the proposed one where we generate a set of images with different masks to indicate different adaptation areas. Feature of each image is extracted by the VGG model. Then, the combined feature will be fed into the RL model. When using the first two types of states, after full training, the RL model still cannot choose the optimal adaptation area for each frame, which demonstrates these states are not suitable for this task. We believe the main reason is that the pre-trained VGG model is able to extract a better feature which contains more information of the original image. Also, the first two ways to indicate the different adaptation areas are not sufficiently explicit and discriminative.

6. Conclusion

In this paper, we have proposed a novel method that can select the best adaptation ROI for each frame to take full advantage of the test time adaptation for video object segmentation. Two RL models are applied to choose the optimal adaptation area for foreground and background individually. Comprehensive experiments on three common benchmark datasets demonstrate the great performance of our method

























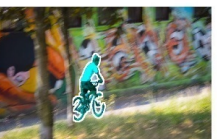





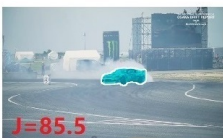














	OnAVOS	RGMP	OSVOS	OURS	GT
camel	 J=74.2	 J=74.6	 J=77.7	 J=92.7	
breakdance	 J=59.5	 J=54.2	 J=68.5	 J=90.9	
motocross jump	 J=77.3	 J=59.1	 J=68.3	 J=88.8	
soapbox	 J=92.5	 J=88.7	 J=63.8	 J=94.8	
bmw-trees	 J=66.2	 J=51.8	 J=54.6	 J=66.4	
dance-twirl	 J=89.8	 J=85.5	 J=87.3	 J=95.4	
drift chicane	 J=85.5	 J=73.3	 J=83.5	 J=90.5	
drift straight	 J=81.9	 J=85.1	 J=54.3	 J=96.3	
scooter black	 J=90.6	 J=88.5	 J=44.8	 J=92.4	

Figure 5: Visualization of segmentation masks and the mean region similarity J_m for different methods on the DAVIS 2016 dataset.

compared with other state-of-the-art methods. In future, we plan to replace the discrete-value actions with the continue-value actions to enable the RL model to find a more flexible way to choose the optimal adaptation ROI.

References

- [1] Asai, K., Yoshio, H., Kato, H., Kaga, T., 2004. Digital video editing method and system.
- [2] Bao, L., Wu, B., Liu, W., 2018. Cnn in mrf: Video object segmentation via inference in a cnn-based higher-order spatio-temporal mrf, in: IEEE Conference on Computer Vision and Pattern Recognition (CVPR).
- [3] Bibi, A., Mueller, M., Ghanem, B., 2016. Target response adaptation for correlation filter tracking, in: European Conference on Computer Vision (ECCV).
- [4] Brutzer, S., Höferlin, B., Heidemann, G., 2011. Evaluation of background subtraction techniques for video surveillance, in: IEEE Con-

- ference on Computer Vision and Pattern Recognition (CVPR).
- [5] Caelles, S., Maninis, K.K., Pont-Tuset, J., Leal-Taixé, L., Cremers, D., Van Gool, L., 2017. One-shot video object segmentation, in: IEEE Conference on Computer Vision and Pattern Recognition (CVPR).
- [6] Chen, Y., Pont-Tuset, J., Montes, A., Van Gool, L., 2018. Blazingly fast video object segmentation with pixel-wise metric learning, in: IEEE Conference on Computer Vision and Pattern Recognition (CVPR).
- [7] Cheng, J., Tsai, Y.H., Hung, W.C., Wang, S., Yang, M.H., 2018. Fast and accurate online video object segmentation via tracking parts, in: IEEE Conference on Computer Vision and Pattern Recognition (CVPR).
- [8] Cheng, J., Tsai, Y.H., Wang, S., Yang, M.H., 2017. Segflow: Joint learning for video object segmentation and optical flow, in: IEEE International Conference on Computer Vision (ICCV).
- [9] Choi, J., Jin Chang, H., Yun, S., Fischer, T., Demiris, Y., Young Choi, J., 2017. Attentional correlation filter network for adaptive visual tracking, in: IEEE Conference on Computer Vision and Pattern Recognition (CVPR).
- [10] Cordts, M., Omran, M., Ramos, S., Rehfeld, T., Enzweiler, M., Benenson, R., Franke, U., Roth, S., Schiele, B., 2016. The cityscapes dataset for semantic urban scene understanding, in: IEEE Conference on Computer Vision and Pattern Recognition (CVPR).
- [11] Danelljan, M., Hager, G., Shahbaz Khan, F., Felsberg, M., 2016. Adaptive decontamination of the training set: A unified formulation for discriminative visual tracking, in: IEEE Conference on Computer Vision and Pattern Recognition (CVPR).
- [12] Deng, J., Dong, W., Socher, R., Li, L.J., Li, K., Fei-Fei, L., 2009. Imagenet: A large-scale hierarchical image database .
- [13] Dong, X., Shen, J., Wang, W., Liu, Y., Shao, L., Porikli, F., 2018. Hyperparameter optimization for tracking with continuous deep q-learning, in: IEEE Conference on Computer Vision and Pattern Recognition (CVPR).
- [14] Everingham, M., Van Gool, L., Williams, C.K., Winn, J., Zisserman, A., 2010. The pascal visual object classes challenge. International Journal of Computer Vision (IJCV) .
- [15] Han, J., Yang, L., Zhang, D., Chang, X., Liang, X., 2018. Reinforcement cutting-agent learning for video object segmentation, in: IEEE Conference on Computer Vision and Pattern Recognition (CVPR).
- [16] Han, Y., Zhang, P., Huang, W., Zha, Y., Cooper, G.D., Zhang, Y., 2019. Robust visual tracking using unlabeled adversarial instance generation and regularized label smoothing. Pattern Recognition .
- [17] Hua, X.S., Lu, L., Zhang, H.J., 2003. Ave: automated home video editing, in: ACM Multimedia.
- [18] Huang, C., Lucey, S., Ramanan, D., 2017. Learning policies for adaptive tracking with deep feature cascades, in: IEEE International Conference on Computer Vision (ICCV).
- [19] Jain, S.D., Grauman, K., 2016. Click carving: Segmenting objects in video with point clicks, in: HCC.
- [20] Jain, S.D., Xiong, B., Grauman, K., 2017. Fusionseg: Learning to combine motion and appearance for fully automatic segmentation of generic objects in videos, in: IEEE Conference on Computer Vision and Pattern Recognition (CVPR).
- [21] Khoreva, A., Benenson, R., Ilg, E., Brox, T., Schiele, B., 2017. Lucid data dreaming for object tracking, in: The DAVIS Challenge on Video Object Segmentation.
- [22] Koh, Y.J., Kim, C.S., 2017. Primary object segmentation in videos based on region augmentation and reduction, in: IEEE Conference on Computer Vision and Pattern Recognition (CVPR).
- [23] Konda, V.R., Tsitsiklis, J.N., 2000. Actor-critic algorithms, in: Conference and Workshop on Neural Information Processing Systems (NIPS).
- [24] Krähenbühl, Philipp, Koltun, V., 2011. Efficient inference in fully connected crfs with gaussian edge potentials, in: Conference and Workshop on Neural Information Processing Systems (NIPS).
- [25] Li, F., Kim, T., Humayun, A., Tsai, D., Rehg, J.M., 2013. Video segmentation by tracking many figure-ground segments, in: IEEE International Conference on Computer Vision (ICCV).
- [26] Li, L.J., Socher, R., Fei-Fei, L., 2009. Towards total scene understanding: Classification, annotation and segmentation in an automatic framework, in: IEEE Conference on Computer Vision and Pattern Recognition (CVPR).
- [27] Li, S., Seybold, B., Vorobyov, A., Fathi, A., Huang, Q., Jay Kuo, C.C., 2018. Instance embedding transfer to unsupervised video object segmentation, in: IEEE Conference on Computer Vision and Pattern Recognition (CVPR).
- [28] Li, Z., Zhong, X., S.Drew, M., 2002. Spatial-temporal joint probability images for video segmentation. Pattern Recognition .
- [29] Liu, Y., Tountas, K., Pados, D.A., Batalama, S.N., Medley, M.J., 2020. L1-subspace tracking for streaming data. Pattern Recognition .
- [30] Luiten, J., Voigtlaender, P., Leibe, B., 2018. Premvos: Proposal-generation, refinement and merging for the davis challenge on video object segmentation 2018, in: IEEE Conference on Computer Vision and Pattern Recognition (CVPR).
- [31] Maninis, K.K., Caelles, S., Chen, Y., Pont-Tuset, J., Leal-Taixé, L., Cremers, D., Van Gool, L., 2017. Video object segmentation without temporal information. arXiv:1709.06031 .
- [32] Märki, N., Perazzi, F., Wang, O., Sorkine-Hornung, A., 2016. Bilateral space video segmentation, in: IEEE Conference on Computer Vision and Pattern Recognition (CVPR).
- [33] Mnih, V., Kavukcuoglu, K., Silver, D., Graves, A., Antonoglou, I., Wierstra, D., Riedmiller, M., 2013. Playing atari with deep reinforcement learning. arXiv:1312.5602 .
- [34] Park, E., Berg, A.C., 2018. Meta-tracker: Fast and robust online adaptation for visual object trackers, in: European Conference on Computer Vision (ECCV).
- [35] Perazzi, F., Khoreva, A., Benenson, R., Schiele, B., Sorkine-Hornung, A., 2017. Learning video object segmentation from static images, in: IEEE Conference on Computer Vision and Pattern Recognition (CVPR).
- [36] Perazzi, F., Pont-Tuset, J., McWilliams, B., Van Gool, L., Gross, M., Sorkine-Hornung, A., 2016. A benchmark dataset and evaluation methodology for video object segmentation, in: IEEE Conference on Computer Vision and Pattern Recognition (CVPR).
- [37] Pont-Tuset, J., Farré, M.A., Smolic, A., 2015. Semi-automatic video object segmentation by advanced manipulation of segmentation hierarchies, in: IEEE Conference on International Conference on ContentBased Multimedia Indexing (CBMI).
- [38] Pont-Tuset, J., Perazzi, F., Caelles, S., Arbeláez, P., Sorkine-Hornung, A., Van Gool, L., 2017. The 2017 davis challenge on video object segmentation. arXiv:1704.00675 .
- [39] Prest, A., Leistner, C., Civera, J., Schmid, C., Ferrari, V., 2012. Learning object class detectors from weakly annotated video, in: IEEE Conference on Computer Vision and Pattern Recognition (CVPR).
- [40] Price, B.L., Morse, B.S., Cohen, S., 2009. Livecut: Learning-based interactive video segmentation by evaluation of multiple propagated cues, in: IEEE International Conference on Computer Vision (ICCV).
- [41] Shankar Nagaraja, N., Schmidt, F.R., Brox, T., 2015. Video segmentation with just a few strokes, in: IEEE International Conference on Computer Vision (ICCV).
- [42] Simonyan, K., Zisserman, A., 2014. Very deep convolutional networks for large-scale image recognition. arXiv:1409.1556 .
- [43] Song, H., Wang, W., Zhao, S., Shen, J., Lam, K.M., 2018. Pyramid dilated deeper convlstm for video salient object detection, in: European Conference on Computer Vision (ECCV).
- [44] Sutton, R.S., McAllester, D.A., Singh, S.P., Mansour, Y., 2000. Policy gradient methods for reinforcement learning with function approximation, in: Conference and Workshop on Neural Information Processing Systems (NIPS).
- [45] Tokmakov, P., Alahari, K., Schmid, C., 2017. Learning video object segmentation with visual memory, in: IEEE International Conference on Computer Vision (ICCV).
- [46] Tsai, Y.H., Yang, M.H., Black, M.J., 2016. Video segmentation via object flow, in: IEEE Conference on Computer Vision and Pattern Recognition (CVPR).
- [47] Voigtlaender, P., Leibe, B., 2017. Online adaptation of convolutional

neural networks for video object segmentation. arXiv:1706.09364 .

- [48] Wang, J., Bhat, P., Colburn, R.A., Agrawala, M., Cohen, M.F., 2005. Interactive video cutout, in: ACM Transactions on Graphics (ACM ToG).
- [49] Wang, T., Han, B., Collomosse, J., 2014. Touchcut: Fast image and video segmentation using single-touch interaction. Computer Vision and Image Understanding (CVIU) .
- [50] Wang, W., Shen, J., Xie, J., Porikli, F., 2017a. Super-trajectory for video segmentation, in: IEEE International Conference on Computer Vision (ICCV).
- [51] Wang, X., 2013. Intelligent multi-camera video surveillance: A review. PRL 34, 3–19.
- [52] Wang, Y., Liu, J., Li, Y., Fu, J., Xu, M., Lu, H., 2017b. Hierarchically supervised deconvolutional network for semantic video segmentation. Pattern Recognition .
- [53] Wu, H., Hu, Y., Wang, K., Li, H., Nie, L., Cheng, H., 2019. Instance-aware representation learning and association for online multi-person tracking. Pattern Recognition .
- [54] Wug Oh, S., Lee, J.Y., Sunkavalli, K., Joo Kim, S., 2018. Fast video object segmentation by reference-guided mask propagation, in: IEEE Conference on Computer Vision and Pattern Recognition (CVPR).
- [55] Xiao, H., Feng, J., Lin, G., Liu, Y., Zhang, M., 2018. Monet: Deep motion exploitation for video object segmentation, in: IEEE Conference on Computer Vision and Pattern Recognition (CVPR).
- [56] Xiao, H., Kang, B., Liu, Y., Zhang, M., Feng, J., 2019. Online meta adaptation for fast video object segmentation. IEEE Transactions on Pattern Analysis and Machine Intelligence (TPAMI) .
- [57] Xie, Y., Xiao, J., Huang, K., Thiyagalingam, J., Zhao, Y., 2018. Correlation filter selection for visual tracking using reinforcement learning. IEEE Transactions on Circuits and Systems for Video Technology .
- [58] Yun, S., Choi, J., Yoo, Y., Yun, K., Young Choi, J., 2017. Action-decision networks for visual tracking with deep reinforcement learning, in: IEEE Conference on Computer Vision and Pattern Recognition (CVPR).